

# PREDICTION OF ENERGETIC PARTICLE CONFINEMENT IN ITER OPERATION SCENARIOS

Z. Lin<sup>1</sup>

<sup>1</sup> University of California, Irvine, CA 92697, USA  
[zhihongl@uci.edu](mailto:zhihongl@uci.edu)

E. Bass<sup>2</sup>, G. Brochard<sup>1,3</sup>, Y. Ghai<sup>4</sup>, N. Gorelenkov<sup>5</sup>, M. Idouakass<sup>6</sup>, C. Liu<sup>5</sup>, P. Liu<sup>1</sup>, M. Podesta<sup>5</sup>, D. Spong<sup>4</sup>, X. Wei<sup>1</sup>, W. Heidbrink<sup>1</sup>, G. McKee<sup>7</sup>, R. Waltz<sup>8</sup>, J. Bao<sup>9</sup>, B. Cornille<sup>10</sup>, V. Duarte<sup>5</sup>, R. Falgout<sup>11</sup>, M. Gorelenkova<sup>5</sup>, T. Hayward-Schneider<sup>12</sup>, S. H. Kim<sup>3</sup>, W. Joubert<sup>4</sup>, S. Klasky<sup>4</sup>, I. Lyngaas<sup>4</sup>, K. Mehta<sup>4</sup>, J. Nicolau<sup>1</sup>, S. D. Pinches<sup>3</sup>, A. Polevoi<sup>3</sup>, M. Schneider<sup>3</sup>, G. Sitaraman<sup>10</sup>, W. Tang<sup>5</sup>, P. Wang<sup>13</sup>, S. Williams<sup>14</sup>

<sup>2</sup> University of California, San Diego, CA 92093, USA

<sup>3</sup> ITER organisation, Route de Vinon-sur-Verdon, CS 90 046 13067 St., Paul Lez Durance, France

<sup>4</sup> Oak Ridge National Laboratory, Oak Ridge, Tennessee 36831, USA

<sup>5</sup> PPPL, Princeton University, Princeton, NJ 08543, USA

<sup>6</sup> National Institute for Fusion Science, 322-6 Oroshi-cho, Toki, Gifu 509-5292, Japan

<sup>7</sup> University of Wisconsin, Madison, Wisconsin 53706, USA

<sup>8</sup> General Atomics, PO Box 85608, San Diego, CA 92186-5608, USA

<sup>9</sup> Institute of Physics, Chinese Academy of Sciences, Beijing 100190, China

<sup>10</sup> AMD, Santa Clara, CA, USA

<sup>11</sup> Lawrence Livermore National Laboratory, USA

<sup>12</sup> Max-Planck-Institut für Plasmaphysik, Boltzmannstr. 2, 85748 Garching, Germany

<sup>13</sup> NVIDIA, Santa Clara, CA, USA

<sup>14</sup> Lawrence Berkeley National Laboratory, USA

## Abstract

Large scale simulations of energetic particle (EP) confinement in the ITER operation scenarios, validated using matching DIII-D experiments, find that macroscopic fishbone can be unstable, but saturate at a low amplitude with insignificant distortion of flux surface and EP re-distribution. Various meso-scale Alfvén eigenmodes (AE) saturate at high amplitudes and drive a large EP transport, which results in a modest flattening of the EP profiles during the short simulation time. Strong microturbulence drives directly little EP transport but large thermal transport, which could affect EP transport driven by the AE and fishbone. These studies point to an optimistic assessment of the EP confinement in the ITER pre-fusion baseline scenario, but also a significant relaxation of the alpha particle profile in the steady state scenario. Therefore, fusion reactor design and scenario development must take into account self-consistent profiles of the alpha and thermal plasmas. Finally, integrated simulation of cross-scale coupling is needed to reliably predict EP confinement in the ITER, as demonstrated in the simulations of the DIII-D experiments.

## 1. INTRODUCTION

EP transport in burning plasmas can be induced by macroscopic MHD modes, meso-scale AE, and microturbulence, which could interact nonlinearly. In this project, EP confinement properties of the ITER operation scenarios have been comprehensively assessed using global gyrokinetic codes (GTC, GYRO, ORB5), kinetic-MHD codes (FAR3D, GAM-solver, M3D-C1, MEGA, NOVA-C, XTOR-K), and reduced EP transport models (CGM, Kick, RBQ). These codes have been first verified and validated for simulations of EP transport in the DIII-D experiments. The comparisons between DIII-D experiments and ITER scenarios provide physics insights on the extrapolation from existing fusion experiments to the future burning plasma experiments. This collaborative research has been selected for US DOE FY2022 Theory Performance Target and adapted as the ITPA energetic particle joint activity B.11.12 project. This paper summarizes key results from this large international collaboration. More detailed results will be reported by other papers [1-4] submitted to this conference.

## 2. PREDICTION OF EP CONFINEMENT IN ITER

After extensive discussions within the EP community, two ITER scenarios: a baseline pre-fusion (BL, shot #101006) and a steady state fusion (SS, shot #131041), have been selected and IMAS equilibrium data have been provided by ITER-IO researchers. To validate the ITER simulations, two

existing DIII-D shots (BL shot #178631, SS shot #132708) with similar safety factors and EP instabilities as the two ITER scenarios have been selected by the DIII-D experimental collaborators. Comprehensive simulations find that the DIII-D and ITER have very similar linear instabilities, thus DIII-D experiments provide an excellent validation for the ITER simulations and for extrapolation from the small DIII-D to the larger ITER.

**Fishbone--** Global gyrokinetic and kinetic-MHD simulations find that fishbone is excited by the NBI EP density gradients and saturates at a low amplitude with insignificant distortion of flux surface and EP re-distribution in the ITER BL as shown in Fig. 1. The simulations have been validated by the excellent agreement of the fishbone mode amplitude and radial structure between simulations and DIII-D ECE measurement of the electron temperature perturbation, as shown in Fig. 2. The fishbone is stable in the ITER and DIII-D SS.

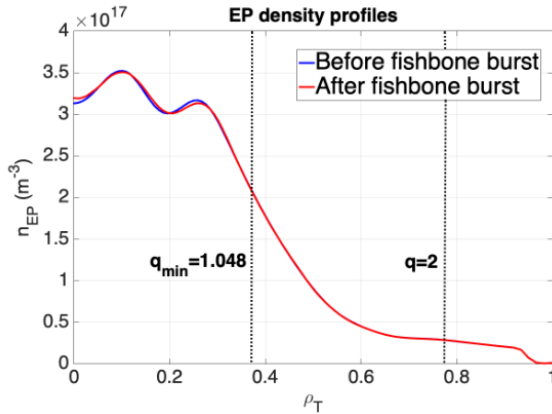


Fig. 1. NBI fast ions density profile before and after fishbone burst in GTC simulation of ITER BL #101006 without zonal flows [1].

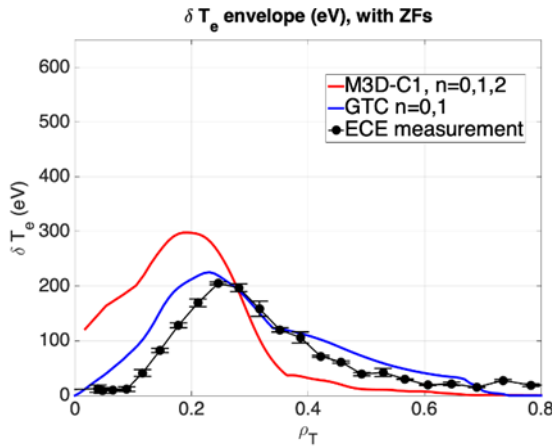


Fig. 2 Radial envelope of electron temperature perturbation  $\delta T_e$  after saturation without in GTC and M3D-C1 simulations of fishbone instability in DIII-D # 178631 [1].

**AE-** Gyrokinetic, kinetic-MHD, and reduced transport model simulations find that beta-induced Alfvén eigenmode (BAE) and reversed-shear Alfvén eigenmode (RSAE) are excited by both NBI and alpha EP density gradients and saturate at high amplitudes in the ITER SS. A strong EP transport is driven, which results in a visible flattening of both the NBI and alpha EP radial profiles in the ITER SS within the short simulation time. AEs are marginally stable or weakly unstable in the ITER BL and DIII-D BL & SS.

Global GTC simulations of the ITER SS #131041 find most unstable beta-induced Alfvén eigenmode (BAE) and reversed-shear Alfvén eigenmode (RSAE) with  $n=[15,30]$  near  $q_{min}$  flux surface, as shown in the left panel of Fig. 3 for the linear eigenmodes. These modes saturate by zonal flows and lead to a strong turbulence with many interacting toroidal modes (right panel).

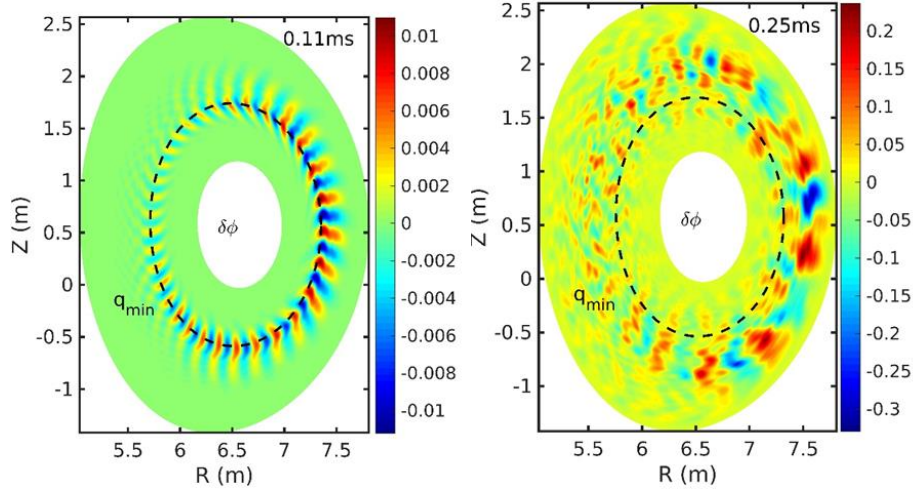
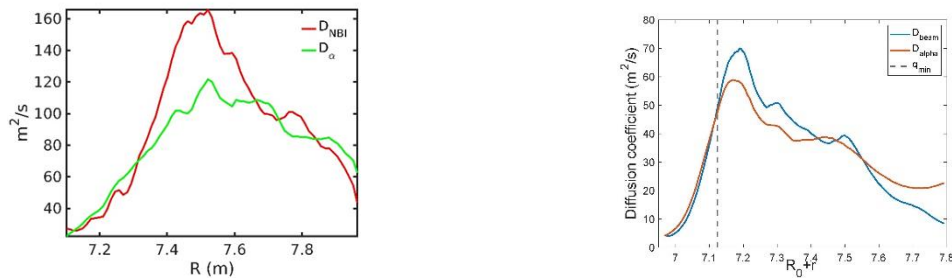


Fig. 3: Poloidal contour plot of electrostatic potential of BAE/RSAE from GTC simulation of ITER SS #131041 for linear eigenmodes (left panel) and nonlinear turbulence (right panel).

The strong AE turbulence drives a huge transport of both alpha and NBI fast ions with a diffusivity  $D$  on the order of  $50 \text{ m}^2/\text{s}$ , as shown in Fig. 4 from gyrokinetic GTC simulations (left panel) and kinetic-MHD MEGA simulation (right panel). The large transport leads to visible profile relaxation in less than 1ms, which has been observed from simulations by GTC, M3D-C1, MEGA, and kinetic-MHD code FAR3D, as shown in Fig. 5.



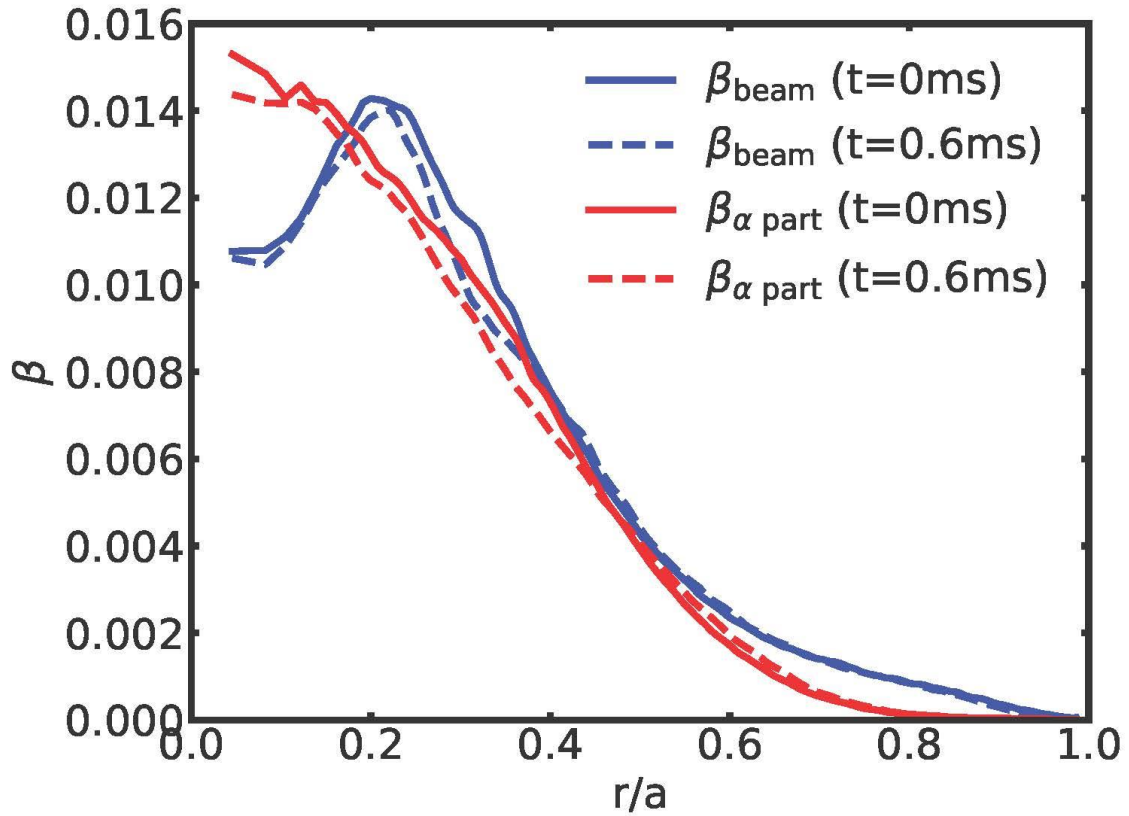


Fig. 4: Radius profiles of NBI beam and  $\alpha$ -particle diffusivities from GTC (left panel) and MEGA (right panel) simulations of AEs in ITER SS.

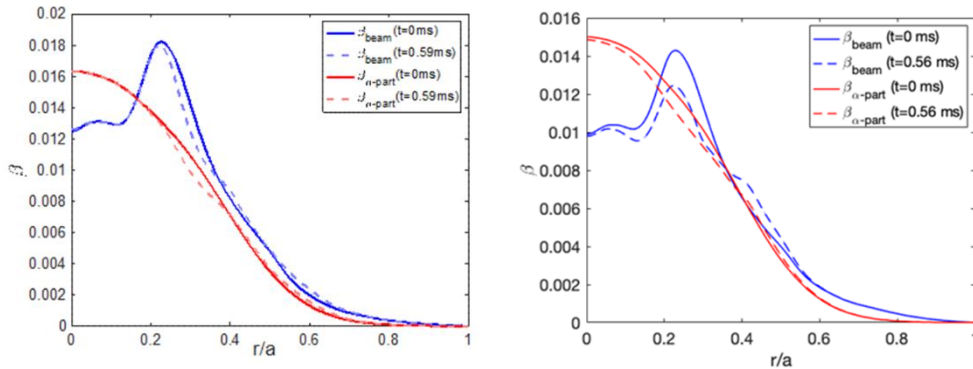


Fig. 5: Relaxation of radius profiles of NBI beam and  $\alpha$ -particle  $\beta$  by AEs from MEGA (left panel) and FAR3D (right panel) simulations of ITER SS [3].

Consistent with first-principles simulations, reduced EP transport models also predict large EP transport and significant EP profile relaxation. The resonance-broadened quasilinear model (RBQ) find EP depletion near magnetic axis due to large diffusion of EP by AEs as shown in Fig. 6. Background microturbulence plays a strong role in EP transport by broadening resonance regions of the wave-particle interaction [6].

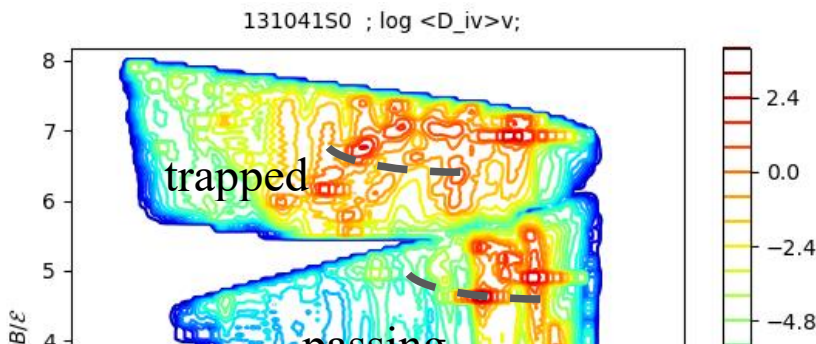


Fig. 6: *RBQ* model showing resonance regions in EP constant of motion phase space with magnetic moment and canonical toroidal momentum. Dash lines are EP diffusion paths in ITER SS.

Another reduced EP transport model, critical gradient model (CGM) TGLF-EP also shows significant relaxation of alpha and NBI fast ions density profiles due to AEs, as shown in Fig. 7. Core-flattening is increased by the microturbulence. The TGLF-EP + Alpha model predicts 30% edge alpha loss when coupled transport and microturbulence is considered.

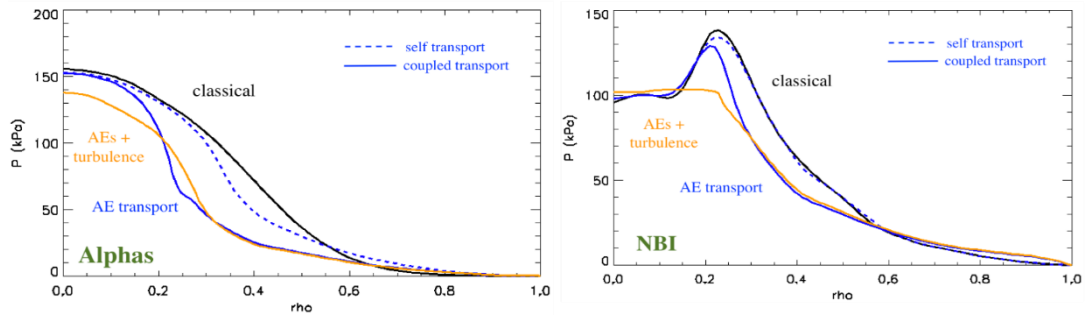


Fig. 7: *Relaxation of radius profiles of a-particle (left panel) and NBI beam (right panel) from CGM simulations of ITER SS [3].*

**Microturbulence--** Gyrokinetic simulations find that strong microturbulence in both SS and BL scenarios of the ITER and DIII-D drives little EP but large thermal transport. Microturbulence could affect AE & fishbone that drive a larger EP transport [5].

Global GTC simulation find strong ion temperature gradient (ITG) instabilities in both ITER SS and DIII-D plasmas. The electrostatic ITG transport satisfies the gyroBohm scaling from the smaller DIII-D to the larger ITER device. Finite- $\beta$  effects reduce the ITG transport in the DIII-D case and the electromagnetic GTC simulation results are consistent with the DIII-D experimental value of the ion heat conductivity as shown in Fig. 8. However, the large- $\beta$  excites kinetic ballooning mode in the ITER SS, which drives huge thermal transport.

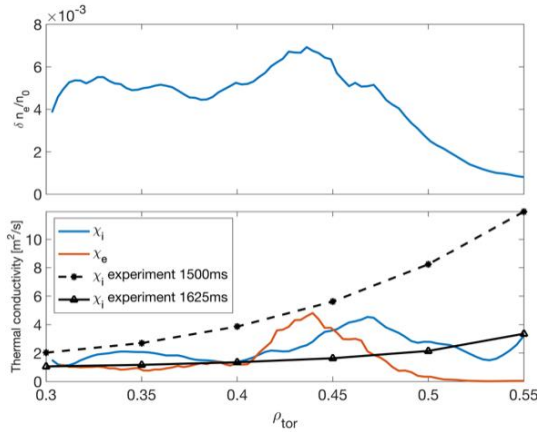


Fig. 8: Radius profiles of electron density perturbation (upper panel) and heat conductivities (lower panel) from GTC simulations of DIII-D #132708. Experimental value of ion heat conductivity is calculated from power balance at two different times.

In summary, these simulations indicate that NBI EP is well confined in the ITER pre-fusion BL scenario, but that both NBI and alpha in the ITER fusion SS scenario could be subjected to significant transport by AEs and profile relaxation. Nonetheless, quantitative prediction of the EP transport needs further integrated simulations coupling MHD, AEs, and microturbulence to incorporate cross-scale interactions.

### 3. NEW EP PHYSICS DISCOVERED THROUGH SIMULATIONS

An exciting finding from global gyrokinetic simulation is that the fishbones in both the DIII-D and ITER BL saturate by zonal flows. Simulations including zonal flows agree quantitatively, for the first time, with the DIII-D experiment regarding mode amplitude and EP transport manifested as neutron emissivity drop. Furthermore, zonal flows generated by the fishbone can suppress thermal plasma transport driven by the microturbulence, consistent with the formation of internal transport barrier after the fishbone bursts in the DIII-D experiment.

Another important physics finding from gyrokinetic, kinetic-MHD, and reduced transport model simulations is that nonlinear interactions of many unstable AEs with a large number of mode rational surfaces lead to a large quasi-steady state EP transport in the ITER SS. Figure 1 shows that GTC gyrokinetic and MEGA kinetic-MHD simulations both find very large NBI and  $\alpha$ -particle diffusivities during a short time scale ( $\sim 0.1\text{ms}$ ) despite very different simulation models. In contrast, EP transport quickly diminishes after AE saturation in the DIII-D experiment where only a few AEs are unstable as shown in gyrokinetic simulations artificially suppressing the microturbulence [5].

### ACKNOWLEDGEMENTS

This collaboration has been coordinated by US DOE SciDAC ISEP Center and by ITPA-EP. Simulations have used DOE INCITE supercomputer time allocation. The views and opinions expressed herein do not necessarily reflect those of the ITER Organization.

### REFERENCES

- [1] G. Brochard et al, Saturation of fishbone modes by self-generated zonal flows in tokamak plasmas, 29<sup>th</sup> IAEA FEC.

- [2] N. Gorelenkov et al, Fast ion relaxation in ITER mediated by Alfvén instabilities using reduced models, 29<sup>th</sup> IAEA FEC.
- [3] D. Spong et al, Energetic particle transport in ITER driven by Alfvénic turbulence, 29<sup>th</sup> IAEA FEC.
- [4] E. Bass et al, Integration of critical-gradient model Alfvén eigenmode-driven energetic ion transport prediction into whole-device modeling workflow for fusion devices, 29<sup>th</sup> IAEA FEC.
- [5] P. Liu *et al.*, *Phys. Rev. Lett.* 128, 185001 (2022).
- [6] V. N. Duarte *et al.*, *Phys. Rev. Lett.* 130, 105101 (2023).